THE JOURNAL OF PHYSICAL CHEMISTRY B

ARTICLE

pubs.acs.org/JPCB

Outstanding Poling Stability of a New Cross-Linked Nonlinear Optical (NLO) Material from a Low Molecular Weight Chromophore

Fabio Borbone,*[,†] Antonio Carella,[†] Antonio Roviello,[†] Mauro Casalboni,[‡] Fabio De Matteis,[‡] Glauco Stracci,[‡] Fabio della Rovere,[§] Andrea Evangelisti,[§] and Massimiliano Dispenza[§]

[†]Dipartimento di Chimica, Università degli Studi di Napoli "Federico II", Complesso Universitario Monte S. Angelo, Via Cintia snc, 80126 Napoli, Italy

[‡]Dipartimento di Fisica, Università di Roma Tor Vergata and INSTM, Via della Ricerca Scientifica 1, 00133 Rome, Italy

[§]Selex Sistemi Integrati, Via Tiburtina KM. 12,400, 00131 Rome, Italy

ABSTRACT: In this paper we report the synthesis and characterization of a trihydroxylated nonlinear optical (NLO) azochromophore and its functionalization with 2,4-tolylendiisocyanate (TDI) to give an amorphous mixture of isomers that was used as a starting compound for the preparation of cross-linked electro-optic (EO) thin films. An unedited type of thermal cross-linking reaction was used, exploiting the reactivity of isocyanate groups themselves in the presence of *N*,*N*-dimethylacetamide, without the addition of any hydroxylated comonomer as usual in the preparation of polyurethanes. Thin films were prepared by spin coating and corona poled during thermal cross-linking. A d_{33} value of 33 pm/V was obtained by second-harmonic generation (SHG) measurements on poled films, and an excellent stability of SHG signal was shown upon aging at 130 °C and during dynamic thermal stability measurements.

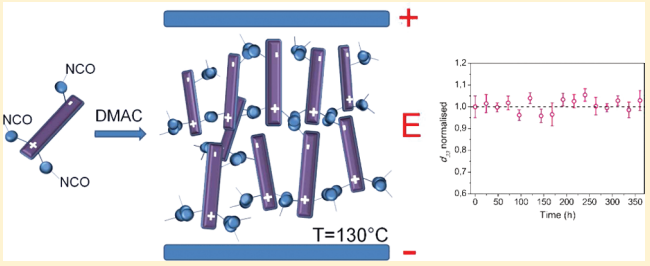

1. INTRODUCTION

Organic and polymeric second-order nonlinear optical (NLO) materials have been a topic of intensive investigation in the last 20 years because they are considered a viable alternative to conventional inorganic crystalline materials for application in electro-optic (EO) devices.[1−4] Organic NLO materials offer in fact, as compared to traditional inorganic ones, some appealing features as lower dielectric constants (which in turn allows better optical to electrical velocity matching, thus higher bandwidth, possibly up to terahertz, to be achieved), higher theoretically achievable EO activity, cheapness in the manufacturing stage, and the possibility, by means of synthetic approaches, of modulating the properties of the materials to match the requirements desired for applications. NLO second-order organic materials are typically based on NLO chromophores embedded in a polymeric matrix and oriented by means of electrical poling in a preferential direction to obtain a noncentrosymmetric arrangement, necessary condition for a material to show second-order nonlinear properties. In recent years, through an intense synthetic effort, chromophores endowed with high values of molecular hyperpolarizability β have been prepared.[5−8] At the same time a careful analysis of the poling process has permitted to optimize the translation of chromophores nonlinear activity into the bulk activity of the materials: specifically, theoretical and experimental works have confirmed that one of the most important factors limiting the efficiency of poling process is represented by the centro-symmetric interactions between dipolar NLO chromophores (and this is especially true when highly active chromophores have to be oriented) and that these interactions could be reduced by modifying the shape of chromophores (a more spherical shape having a positive influence on poling efficiency)[9,10] or by trying to isolate them in the polymeric matrix (that eventually could result in a dendritic approach).[11,12] Following these guidelines, materials with r_{33} higher than 300 pm/V (well higher than r_{33} value of 30 pm/V showed by lithium niobate) have been reached,[13,14] and devices with modulation bandwidths of hundreds of gigahertz and operating at digital driving voltages have been fabricated.[15]

However, even if excellent activities have been achieved, the rapid development of EO organic devices is hindered by several problems, like the not yet excellent temporal stability of NLO activity: unlike conventional inorganic materials, organic systems suffer in fact a loss of activity with time span due to the relaxation of chromophore alignment obtained through electrical poling. Different approaches have been investigated to face with this problem, such as hybrid organic−inorganic systems[16,17] or high glass transition temperature (T_g) polymeric systems containing NLO chromophores as guest molecules or covalently linked.[18−22] The main problem of this kind of systems is the necessity of orienting chromophores at very high temperatures (poling temperature should be around T_g of the polymer) that could result in degradation of chromophores. Polymers characterized

Received: May 16, 2011
Revised: September 12, 2011
Published: September 15, 2011

Scheme 1. Synthesis of $DMOH_3$, DMI_3, and $DMAc_3$

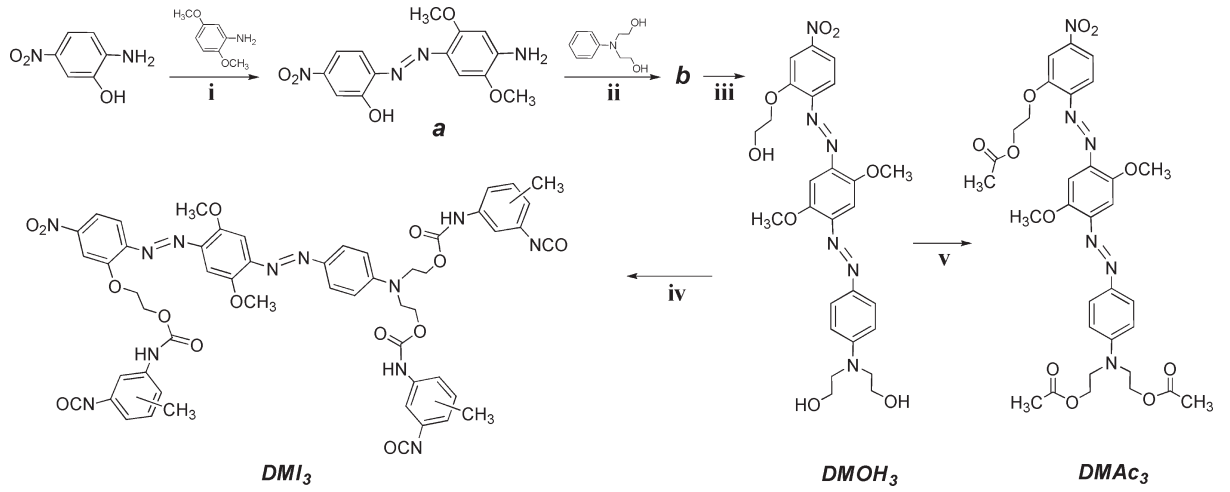

i: $NaNO_2$, HCl, 0−5 °C; **ii**: $NaNO_2$, HCl, NaCl, $ZnCl_2$, 0−5 °C; **iii**: K_2CO_3, $Br(CH_2)_2OH$, DMF, rt; **iv**: TDI, THF, rt; **v**: Ac_2O, Py, reflux.

by networking functionalities have also been synthesized and networking triggered during the poling process to hardly hinder chromophore relaxation.[23−26] Based on the same idea, chromophores functionalized for networking reaction have been synthesized with a low tendency to crystallize to give amorphous films: thin films of these chromophores have been poled and networked, giving stable NLO materials.[27−29] By means of this approach, it is reasonably possible to obtain materials with a high degree of chromophore alignment, since the orientation is performed when the chromophores are not yet fully bound to the macromolecular system. At the same time high time stability of the polar order could be achieved because of the networking. Up to date the retention of around 90 % of NLO activity after baking the device for hundreds of hours at 85 °C has been achieved; this temporal stability has to be unquestionably enhanced to allow the commercialization of organic devices.

In this work we report on a trifunctionalized NLO chromophore which has been poled and cross-linked at the same time, leading to a material with NLO activity comparable to that of lithium niobate and an outstanding temporal stability of the nonlinear response with temperature. To obtain the networkable system, chromophores have been functionalized with isocyanate moieties. In previous reports[30] this kind of functionalization has already been exploited for the realization of a stable network, whereas the triisocyanate chromophores were reacted with precross-linked mixtures of diisocyanates/triols, thus obtaining a guest−host approach that lead to a typical polyurethane network. Here we describe a new cross-linking mechanism involving the isocyanate end groups of the chromophores, which is independent from the use of di- or polyol comonomers and hence leads to a new type of network with optimal properties. Moreover, no further dilution of the NLO active species occurs within the material, and no more than one component is needed for the deposition of the cross-linkable mixture. We reckon that this kind of processing discussed hereafter has the appealing feature of generality, being applicable to different NLO chromophores, and leading, as we will show, to materials with an unprecedented temporal stability of NLO activity.

2. EXPERIMENTAL SECTION

2.1. Synthesis. A trifunctionalized azo-chromophore containing three ethanol groups as pendants was easily synthesized ($DMOH_3$, Scheme 1) by diazotation of 2-amino-5-nitrophenol and copulation onto 2,5-dimethoxyaniline. The intermediate **a** was further diazotated and copulated onto *N*,*N*-diethanolaniline to give the trihydroxylated chromophore **b** that was alkylated on the phenolic hydroxyl with 2-bromoethanol to give $DMOH_3$. This and similar molecules can be easily functionalized by a reaction with asymmetrical diisocyanates to give uncrystallizable mixtures of triisocyanate isomers that can be precipitated and directly used for spin coating of amorphous thin films without further reactions. Hence $DMOH_3$ was reacted with excess 2,4-tolylenediisocyanate to give a mixture of isomers DMI_3 that was used as a starting compound for the preparation of the cross-linked second-order NLO material. The chromophore $DMOH_3$ was also acetylated to give $DMAc_3$ which was used as the model compound for linear and nonlinear optical characterization.

2-Amino-5-nitrophenol, 2,5-dimethoxyaniline, *N*,*N*-diethanolaniline, 2-bromoethanol, and 2,4-tolylendiisocyanate (TDI) are commercially available. All commercial products and solvents were used without further purification, except for TDI which was distilled under vacuum.

(E)-2-((4-Amino-2,5-dimethoxyphenyl)diazenyl)-5-nitrophenol (***a***). A total of 15.0 g (97.3 mmol) of 2-amino-5-nitrophenol was suspended in 165 mL of water and 53 mL of 37% wt HCl. The mixture was cooled at 0−5 °C, and 6.74 g (97.3 mmol) of $NaNO_2$ in 50 mL of water was added under stirring. After 2 h the diazonium salt was isolated by vacuum filtration. The diazonium salt was slowly added to a solution of 14.9 g (97.3 mmol) of 2,5-dimethoxyaniline in 200 mL of a solution containing 20 mL of 37% wt HCl, 40 mL of ethanol, and 140 mL of water. After 1 h under stirring the mixture was poured into 500 mL of water saturated with sodium acetate. A green solid (**a**) was isolated by filtration and recrystallized from acetone/heptane (1:3). Yield: 77%. Mp: 218 °C.

^{1}H NMR ($CHCl_3$-*d*) δ (ppm): 3.916 (s, 3H); 3.951 (s, 3H); 4.684 (s, 2H); 6.316 (s, 1H); 7.781 (s, 1H); 7.852 (m, 3H); 13.861 (s, 1H).

2,2′-(4-((E)-(4-((E)-(2-Hydroxy-4-nitrophenyl)diazenyl)-2,5-dimethoxyphenyl)diazenyl)phenylazanediyl)diethanol (***b***). A total of 5.00 g (15.8 mmol) of the product **a** was triturated and suspended in 500 mL of water and 75 mL of 37% wt HCl. A solution containing 42.5 g (311 mmol) of $ZnCl_2$ and 18.2 g (311 mmol) of NaCl in 50 mL of water was added, and the suspension was cooled to 0−5 °C. A sample of 5.00 g (72.6 mmol) of $NaNO_2$ in 10 mL of water was added under stirring, and the mixture was left warming to room temperature. After 24 h a green solid was filtered in vacuo. The diazonium salt was added at room temperature to a solution containing 11.5 g (63.3 mmol) of *N,N*-diethanolaniline in 100 mL of dimethylformamide (DMF). After 12 h under stirring the solution was poured into 300 mL of water saturated with sodium acetate. A dark solid (**b**) was filtered in vacuo, washed with water, and recrystallized from boiling tetrahydrofuran (THF)/hexane (50/50). Yield: 71%.

^{1}H NMR (Py-d_5) δ (ppm): 3.90 (m, 10 H); 4.09 (t, 4H, J = 5.4 Hz); 7.04 (d, 2H, J = 9.4 Hz); 7.74 (s, 2H); 7.85 (d, 1H, J = 12.2 Hz); 8.08 (s, 1H); 8.09 (s, 1H, J = 12.2 Hz); 8.22 (d, 2H, J = 9.4 Hz).

2,2′-(4-((E)-(4-((E)-(2-(2-Hydroxyethoxy)-4-nitrophenyl)diazenyl)-2,5-dimethoxyphenyl)diazenyl)-phenylazanediyl)diethanol (DMOH$_3$). A total of 8.00 g (15.7 mmol) of product **b** was dissolved in 100 mL of DMF containing 5.00 g (36.2 mmol) of K_2CO_3. A sample of 9.81 g (78.5 mmol) of 2-bromoethanol was slowly added under stirring. After 72 h the solution was filtered and precipitated in 300 mL of water saturated with sodium acetate. The product ($DMOH_3$) was filtered, recrystallized from boiling THF/hexane, and purified by chromatography (Florisil 60/100, THF). Yield: 85%.

^{1}H NMR (DMSO-d_6) δ (ppm): 3.21 (t, 4H); 3.46 (t, 4H); 3.71 (t, 2H); 3.79 (s, 3H); 3.85 (s, 3H); 4.23 (t, 2H, J = 4.5 Hz); 4.75 (s, 2H); 4.88 (s, 1H); 6.75 (d, 2H, J = 8.7 Hz); 7.23 (s, 1H); 7.24 (s, 1H); 7.46 (d, 1H, J = 8.7 Hz); 7.65 (d, 2H, J = 8.7 Hz); 7.79 (d, 1H, J = 8.7 Hz); 7.93 (s, 1H). Calcd for $C_{26}H_{30}N_6O_8$: C, 56.31; H, 5.45; N, 15.15. Found: C, 56.29; H, 5.37; N, 15.21.

DMI$_3$. A total of 0.500 g of $DMOH_3$ (0.902 mmol) was dissolved in 30 mL of dry nonstabilized THF containing 4 mL of distilled TDI. After 15−17 h under stirring at room temperature the product was precipitated in 200 mL of dry heptane, filtered, and vacuum-dried. Yield: 98%. The ^{1}H NMR analysis of the mixture of isomers in DMSO-d_6 shows the disappearing of hydroxyl signals at 4.75 and 4.88 ppm and the appearance of multiple signals of TDI in the region of 7 ppm, whose integration corresponds to 9 protons.

DMAc$_3$. A sample of 0.500 g of $DMOH_3$ (0.902 mmol) was refluxed for 1 h in 30 mL of dry pyridine containing 0.552 g (5.41 mmol) of acetic anhydride. The product was precipitated in 100 mL of water, filtered, washed, and purified by column chromatography. ^{1}H NMR (DMSO) δ (ppm): 1.99 (s, 9H); 3.75 (m, 4H); 3.93 (s, 3H); 3.97 (s, 3H); 4.22 (t, 4H); 4.52 (t, 4H); 6.97 (d, 2H); 7.36 (s, 2H); 7.62 (d, 1H); 7.80 (d, 2H); 7.95 (dd, 1H); 8.05 (d, 1H).

Monomer pretreatment was carried out by dissolving 100 mg of DMI_3 in 1 mL of THF and 70 mg of *N,N*-dimethylacetamide and stirring for 15 min at room temperature. The solution was then filtered on 0.2 μm Teflon filters and spin-coated at 800 rpm for 120 s onto glass slides.

2.2. Instrumentation. Optical observation was performed by using a Zeiss Axioscop polarizing microscope equipped with a FP90 Mettler heating stage. Thermal properties were measured using a differential scanning calorimeter (DSC) Perkin-Elmer Pyris 1 with a scanning rate of 10 °C/min, under nitrogen flow.

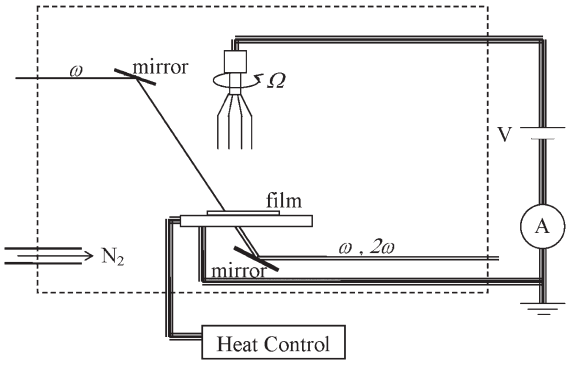

Figure 1. Scheme of the corona poling setup. V: voltage source. A: amperometer. Ω: angular speed of the tips. ω: fundamental frequency. 2ω: second harmonic frequency.

UV−vis absorption spectra were recorded at room temperature by use of a Jasco V-560 spectrophotometer. Thermogravimetric analyses were performed in nitrogen and air by a TA Instruments SDT 2960 Simultaneous DTA-TGA. The structures of chromophores and intermediates were confirmed by ^{1}H NMR. The spectra were recorded using Varian spectrometers operating at 200 and 300 MHz. IR spectra were recorded on a FT/IR-430 JASCO spectrophotometer. The molecular quadratic optical nonlinearities of the chromophore $DMAc_3$ was experimentally determined by the EFISH technique. The setup allows the determination of the scalar $\mu\beta$ product where μ is the dipole moment and β the vector part of the quadratic hyperpolarizability tensor. The measurements were performed at 1.907 μm and calibrated relative to a quartz wedge whose quadratic susceptibility, $d_{11} = 1.2 \times 10^{-9}$ esu at 1.064 μm, was extrapolated to 1.1×10^{-9} esu at 1.907 μm.

Thin polymeric films were deposited from solution by means of a SCS P6700 spin coater. The film thickness and refractive index were measured by a variable angle spectroscopic ellipsometer (VASE J.A. Woollam Co.) which exploits the rotating analyzer configuration. The setup is equipped with a computer-controlled retarder (AutoRetarder) which allows the analysis of ellipsometric angles in the range 0−360°. The measurable spectral range is 190−1700 nm. The films thickness was measured also with an Alphastep 200 profilometer.

The experimental setup used for chromophore orientation is a conventional corona poling setup. The ionization of the atmosphere gas is caused by the strong electric field created at eight sharp copper tips placed at a high electric potential (of the order of kilovolts) at a distance of 4 cm over a metallic plate which works as a ground electrode and, at the same time, as a sample holder and a heater. A sketch of the apparatus is shown in Figure 1.

An external control of the electrical current between the electrodes is established to have a constant electric field across the sample. The setup is electrically isolated in a nitrogen atmosphere to control the humidity and, consequently, to limit the flow of electric charges toward the sample. The eight tips produce a large coverage of the sample by the poling field yielding a homogeneous noncentrosymmetric material without damage, as verified by measuring the $d_{33}(0)$ coefficient in several different places of the sample. This is an important feature since the manufacturing of EO devices requires large and homogeneous poled areas (of the order of several cm^2).

The nonlinear optical measurements have been performed by means of a Q-switched Nd:YAG laser acting as the pump of an

optical parametric oscillator (OPO), whose wavelength can be tuned in the near-infrared range (800−1600 nm). The fundamental wavelength was set to 1500 nm, out of absorption resonance for the material both in the fundamental and the second-order harmonics. A potassium dideuterophosphate (KDP) crystal was used to generate a reference second harmonic (SH) signal from the fundamental beam reflected by a beam splitter cube, to take into account of the power fluctuations of the fundamental laser beam. A double Fresnel rhomb selected the proper polarization direction (*s* or *p*) for the fundamental beam impinging on the sample, which was placed on a goniometric stage to allow variation of the angle of incidence. The signals were detected by photodiodes and acquired by a computer interfaced digitizing oscilloscope. The insertion of a combination of mirrors allows the performance of in situ SHG measurements during the poling procedure (Figure 1).

3. RESULTS AND DISCUSSION

The tri-isocyanate derivative DMI_3 shows high solubility in chloroform, dichloromethane, THF, or dioxane and can be easily spin-coated in several conditions, leading to amorphous thin films with thickness up to some micrometers for highly concentrated solutions. Cross-linking of these films is observed upon heating as a consequence of reactions involving isocyanate and/or urethane groups attached on the molecules. Thermal treatment at 160 °C for 2 h is sufficient to completely cross-link the material and make it insoluble in strong solvents like DMF. However, by following this procedure, problems of stability arise during the process of corona poling, where bleaching and complete erosion of the sample is observed after few minutes from voltage application while heating. This behavior is evidently related to the poor resistance of the film surface to the ionic flow generated by the corona wire, in conditions where the material is predominantly a mixture of low molecular weight fractions and no significant degree of polymerization has been yet reached. In our experimental conditions DMI_3 was dissolved in THF (100 mg/mL) and spin-coated after 15 min at room temperature onto glass substrates. According to the literature, in this poorly polar solvent at room temperature no significant reactions occur between urethane and isocyanate functions, so that deposited material can be reasonably assumed to be constituted only of unreacted molecules. An early prepolymerization (needed to sufficiently harden the material, thus solving the problem of erosion) requires a thermal treatment at 170 °C for at least 1.5 h before voltage application. This behavior is consistent with observations of Lapprand et al.[31] who have demonstrated that urethane and isocyanate functions react slowly only at high temperatures giving mainly allophanates. Nevertheless, when samples were subjected to this procedure, only poor chromophore orientation and hence low nonlinear response was observed; in addition, the system showed fast time decay of second-order activity, probably because of a relative instability of allophanate cross-linking. The best approach to avoid thermal pretreatment and enhance NLO response seemed to be the use of reactive solvents with catalytic properties like *N*,*N*-dimethylacetamide (DMAC). It is known that DMAC reacts with isocyanates giving *N*,*N*-dimethylacetamidines whose further reaction leads to the formation of carbamides and cyclic products like isocyanurates, substituted barbituric acids, and aminouracils.[32,33] Some of these reactions occur at a significant rate even at room temperature due to the catalytic effect of DMAC itself. In fact

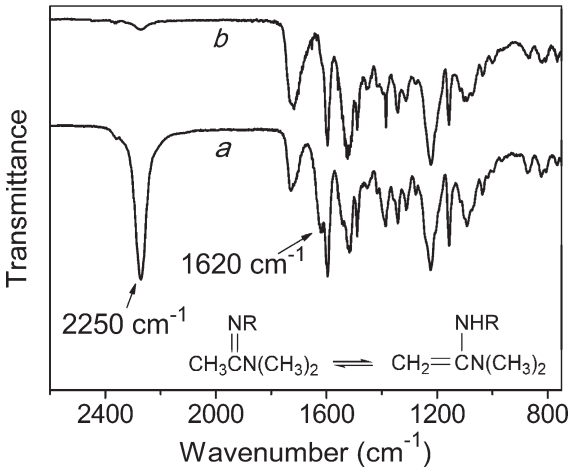

Figure 2. FT-IR analysis of DMI_3 thin film before (a) and after (b) the curing at 160 °C for 2 h.

rapid cross-linking of compound DMI_3 was observed when it was dissolved in DMAC after few hours. Furthermore spin-coated films from the DMAC result nearly insoluble just after deposition and could not reach appreciable degree of orientation during poling. The best poling/cross-linking conditions were found by adding small amounts of DMAC to THF (dichloromethane) solutions of monomers and stirring at room temperature for 15 min before spin coating. This treatment resulted enough to preharden the material to a minimum extent to avoid surface erosion during corona poling, granting at the same time optimal chromophore orientation and nonlinear response. This cross-linking path also ensures outstanding time stability of NLO properties as described hereafter. Although several mono- and dialkyl-formamides/acylamides were successfully tested, samples treated with DMAC had the best performance both in terms of poling efficiency and time stability of optical nonlinearity.

The FT-IR analysis of a spin-coated film (Figure 2) before (a) and after (b) the thermal treatment (160 °C for 2 h) shows the strong decrease of the isocyanate peak (2250 cm^{-1}). One more evident effect is the disappearing of the absorption at 1620 cm^{-1}. This peak can be reasonably assigned to the C═N/C═C stretching relative to the acetamidines that form because of the reaction between DMAC and isocyanate functions during the initial stage at room temperature:

However, several other side reactions can occur between isocyanate functions where DMAC acts as reactant or simply as a catalyst, as demonstrated by Matsui et al.[32] Most of them seem to lead to cyclic species where more than two chromophore pendants could be involved and tied together, resulting in a highly thick network. One of the advantages with this cross-linking approach is also the curing rate, which in our experimental conditions resulted suitable for an optimal alignment of chromophores during electrical poling. To study the behavior of the material in poling conditions, thin films were prepared by spin coating deposition on glass slides as described in the Experimental Section and poled by using the experimental setup illustrated in Figure 1. The best poling conditions, corresponding to higher nonlinear response, were found by first applying an electrode voltage of 7 kV, heating the samples as rapidly as possible (∼3 min) to 160 °C and keeping it at this temperature for 2 h. This time is long enough in practice for the completion of the hardening process, as shown in the DSC diagram (Figure 3)

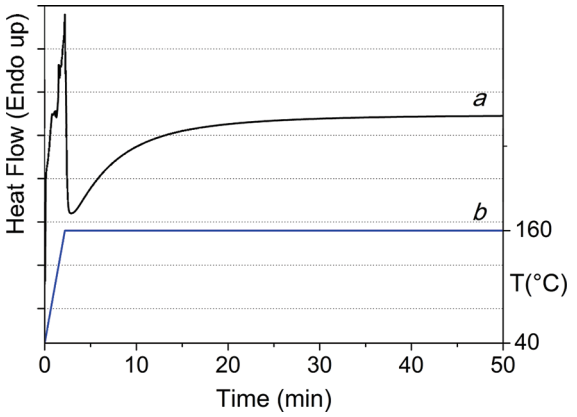

Figure 3. DSC thermogram of DMI_3 (a) during the temperature ramp (b).

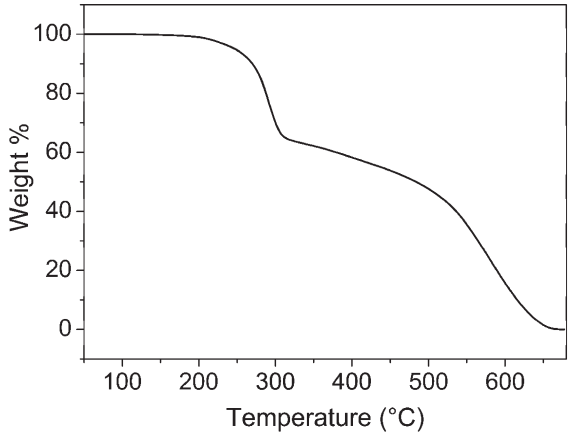

Figure 4. Thermogravimetric analysis of DM-c.

recorded as a function of time, where the curve reaches a plateau after the exothermic peak due to the cross-linking reaction.

The experimental setup allowed us to observe the second harmonic (SH) signal during the thermal program. The SH intensity rapidly increases at lower temperatures during the heating ramp because the increasing chromophore mobility promotes the orientation. As the temperature approaches 160 °C the signal falls to zero, the applied electric field not being strong enough to overcome the molecular disorientation caused by thermal energy. After some minutes the SH signal starts again to grow slowly to approximately the same maximum intensity reached during the heating ramp, as a consequence of the polymerization and formation of the network involving a progressive increase of the glass transition temperature of the material during the hardening process. This behavior demonstrates that this cross-linking mechanism requires high temperatures to proceed at a significant rate, hence allowing a better control over the poling process because the chromophore orientation is not hindered by a rapid decrease of their mobility, due to the network formation, during the early stage of the electrical poling. After the completion of curing the samples were cooled down to room temperature and the voltage removed. The cross-linked material (DM-c) has a high thermal stability, as demonstrated by the thermogravimetric analysis recorded in air (Figure 4) on a thin film poled sample whose decomposition temperature, measured at 5% weight loss, is about 247 °C.

Table 1. Absorption Data of $DMAc_3$

solvent	μ^a (D)	$\lambda_{max}{}^b$ (nm)	$\lambda_{cutoff}{}^c$ (nm)	$\varepsilon^d/10^4$ ($L \cdot cm^{-1} \cdot mol^{-1}$)
ethyl acetate	1.78	542	656	4.2
acetone	2.88	543	666	4.2
N,*N*-dimethylacetamide	3.81	555	687	4.3
DMSO	3.96	562	704	4.2

[a] Solvent dipole moment by *Handbook of Chemistry and Physics*, 59th ed.; CRC Press, Inc: Boca Raton, FL. [b] Wavelength of UV−vis absorbance maximum. [c] Wavelength at 5% of absorbance maximum. [d] Molar absorbance coefficient.

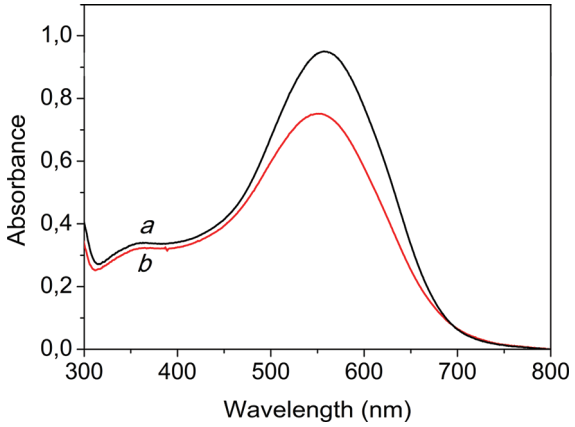

Figure 5. Electronic spectrum of DMI_3 thin film before (a) and after (b) poling/cross-linking.

The model chromophore $DMAc_3$ and thin films of the pretreated tri-isocyanate derivative before and after poling/cross-linking were characterized for their linear and nonlinear optical properties. Some relevant absorption data from UV−vis spectrum of $DMAc_3$ in several solvents are reported in Table 1. The absorption range is situated below the typical wavelengths used for EO applications as well as the fundamental and SH wavelengths adopted for nonlinear optical characterization. A very similar electronic spectrum is observed for a thin film (Figure 5), whose absorption maximum slightly shifts from 557 to 551 nm upon poling/cross-linking, and a decrease of the maximum absorbance is recorded as a consequence of chromophore orientation. The corresponding orientational order parameter[34] for poled materials is 0.21, calculated from the expression $\phi = 1 - A_\perp/A_0$, where $A_\perp$ is the absorbance at λ_{max} of the poled sample (with the incident beam polarization perpendicular to the poling direction) and A_0 is the absorbance at λ_{max} of the unpoled film. The determination of molecular optical nonlinearity was realized by measuring the $\mu\beta$ coefficient of $DMAc_3$ through the EFISH technique on chloroform solution. The chromophore shows a value of 1900×10^{-48} esu, which was slightly lower if compared with that of the chromophore M_{1Mod} previously reported in the literature[35] and had a chemical structure similar to $DMAc_3$ except for the alkoxy group on the nitrophenyl ring. This group has apparently a detrimental effect on the electronic structure, acting as an additional donor placed near the electron acceptor group. Nevertheless, the presence of this further anchoring function on the other end of the molecule could be considered a crucial factor to efficiently and permanently keep the chromophores alignment within the cross-linked material.

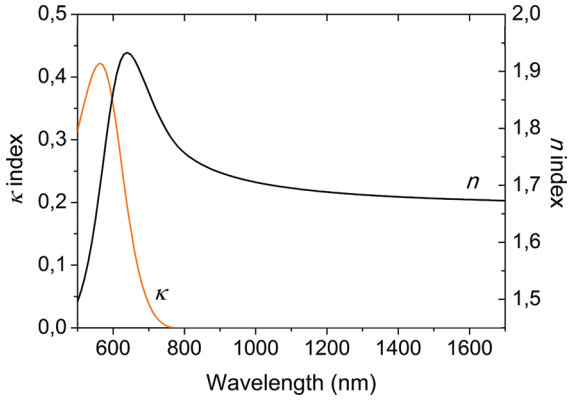

Figure 6. Spectral dispersion for real (n) and imaginary (κ) parts of the refractive index.

Second-order NLO response was determined by measuring the d_{33} component of nonlinear second-order optical susceptibility $\chi^{(2)}$ on poled films by means of the Maker fringes technique.[36,37] Measurements of the SH signal generated by the sample ($P_{2\omega}$) were recorded as a function of the angle of incidence along with incident power (P_ω), and data were best fitted according to the Herman and Hayden SH power equation:[38]

$$\frac{P_{2\omega}^{\gamma \rightarrow p}}{P_\omega^2} = \frac{128\pi^3}{cA}\left(\frac{2\pi L}{\lambda}\right)^2 \frac{[t_{af}^{1\gamma}]^4[t_{fs}^{2p}]^2[t_{sa}^{2p}]^2}{n_{2\omega}^2 \cos^2\theta_{2\omega}} d_{eff}^2 \exp[-2(\delta_1 + \delta_2)] \times \frac{\sin^2\Psi + \sinh^2\chi}{\Psi^2 + \chi^2}$$

where A is the cross-sectional area of the fundamental beam, λ is its wavelength, θ is the angle of incidence, L is the film thickness, n_ω and $n_{2\omega}$ are the refractive indices of the fundamental and SH waves, $t_{af}^{1\gamma}$, t_{af}^{2p}, and t_{sa}^{2p} are the Fresnel transmission coefficients for the air/film, film/substrate, and substrate/air interfaces, θ_ω and $\theta_{2\omega}$ are such that $\sin\theta_\omega = \sin\theta/n_\omega$ and $\sin\theta_{2\omega} = \sin\theta/n_{2\omega}$, and Ψ and χ are given by the expressions:

$$\Psi = \frac{2\pi L}{\lambda}(n_\omega \cos\theta_\omega - n_{2\omega}\cos\theta_{2\omega})$$

$$\chi = \delta_1 - \delta_2 = \frac{2\pi L}{\lambda}\left(\frac{n_\omega \kappa_\omega}{\cos\theta_\omega} - \frac{n_{2\omega}\kappa_{2\omega}}{\cos\theta_{2\omega}}\right)$$

where κ_ω and $\kappa_{2\omega}$ are the extinction coefficients of the material at the fundamental and SH frequencies. All of the constant terms were included in a constant K that was determined by calibration with 1 mm thick x-cut quartz plate ($d_{11} = 0.30$ pm/V)[39] fitting $P_{2\omega}/(P_\omega)^2$ measured for quartz as a function of the incident angle.

Thickness and spectral dispersion measurements of DM-c samples were performed with a spectroscopic ellipsometer with a wavelength resolution of ± 0.03 nm. The refractive index was obtained fitting the experimental ellipsometric data to a Cauchy model in the spectral region far apart from the absorption resonance wavelength[40] and to a Tauc−Lorentz model in the region of absorbance.[41]

Figure 6 shows the spectral dispersion for real and imaginary part of the refractive index. First we can observe that the refractive index is 1.66 at the fundamental wavelength (1500 nm),

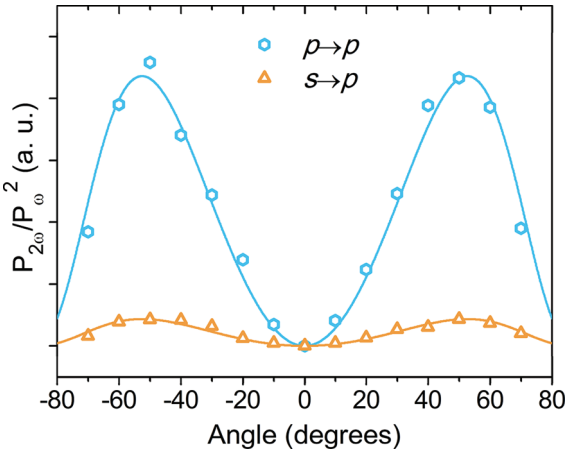

Figure 7. Maker fringe patterns of SH signal for DM-c poled film. Circles ($p\rightarrow p$) and triangles ($s\rightarrow p$) are experimental data; full-line curves are best fit.

while it is 1.79 at the SH wavelength (750 nm). The thickness of the polymeric film is 940 nm. We can also see that, even at the SH frequency, the extinction coefficient is as low as 3×10^{-3} and the influence on the nonlinear coefficient should be not relevant.

The d_{33} component for DM-c can be gathered from a $p\rightarrow p$ experiment ($\gamma = p$, p-polarized incident beam → p-polarized component of SH signal recorded) being:[38]

$$d_{eff} = d_{15}\cos\theta_{2\omega}\sin 2\theta_\omega + d_{31}\cos^2\theta_\omega \sin\theta_{2\omega} + d_{33}\sin^2\theta_\omega \sin\theta_{2\omega}$$

once the sample thickness and refractive index at the fundamental and SH wavelengths are known from the ellipsometric data and the relations $d_{31} = d_{15}$ (Kleinmann symmetry condition[42]) and $d_{31} = 1/3 d_{33}$ are used.[43] Figure 7 shows the Maker fringes for DM-c:

The best fit gives for d_{33} a value of 33.0 pm/V, as much as d_{33} coefficient of lithium niobate, one of the reference materials for nonlinear optics. A further measurement with the s-polarized incident beam ($s\rightarrow p$) allowed to separately determine d_{31} component being in this case:[38]

$$d_{eff} = d_{31}\sin\theta_{2\omega}$$

The best fit gives a value of 10.8 pm/V, confirming that the condition $d_{31} = d_{33}/3$ used for $p\rightarrow p$ fitting represents a good approximation.

To evaluate the loss of NLO activity with time due to progressive relaxation of the induced alignment, poled thin films of DM-c were baked in air at several temperatures, and the SH signal was periodically recorded. Regardless of the extent of the second-order nonlinear response, this material possesses excellent stability of NLO properties with time, as it can be evinced from Figure 8, reporting the best result at the highest temperature (130 °C) where no sensible decrease of d_{33} coefficient can be observed, within the experimental error, after thermal treatment of a poled sample.

The same sample has maintained the SH signal unaltered after one year on the shelf. The nonlinear response stability of DM-c poled films was also tested in a dynamic temperature-dependent experiment, performed in the apparatus of Figure 1 by measuring the SH signal while the samples were heated at 3 °C/min in air.

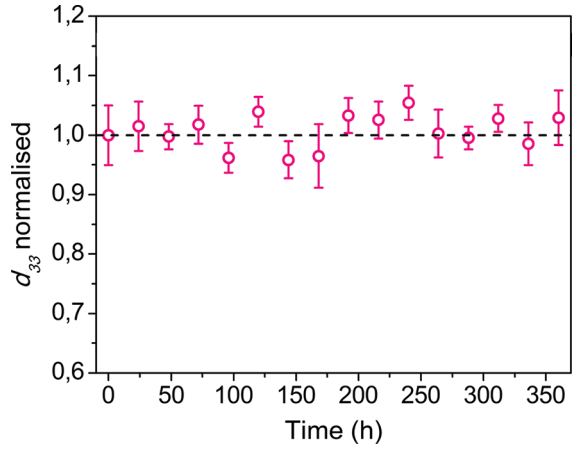

Figure 8. Normalized d_{33} coefficient of DM-c after aging in air at 130 °C.

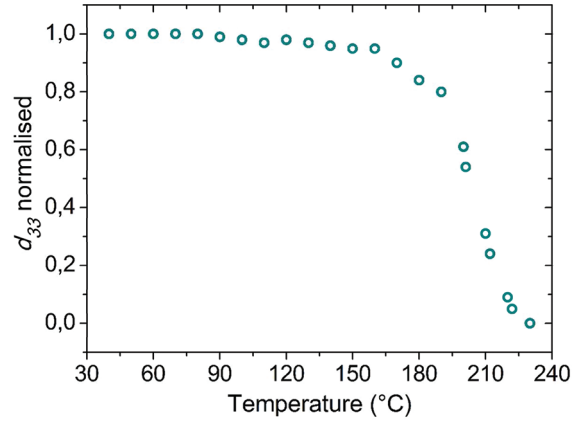

Figure 9. Normalized d_{33} coefficient of DM-c during heating in air at 3 °C/min.

The results are shown in Figure 9 and reported as normalized nonlinear coefficient.

The graph shows a typical trend where the nonlinearity undergoes a slight diminution with the increasing temperature, followed by a rapid and irreversible decline due to thermal decomposition and/or depoling effects. From Figure 9 the limit of dynamic thermal stability for poled DM-c can be identified at about 160 °C, corresponding to the cross-linking temperature of the material in our experimental conditions. These results confirm the outcome of thermal aging tests, which is the capability of DM-c to keep its NLO activity almost unchanged at significantly high temperatures. This outstanding stability can be ascribed to a very efficient hardening process involving the formation of a highly thick network, combined with a molecular structure characterized by a large fraction of rigid moieties that contribute to a marked reduction of chromophore mobility within the final network. The likely formation of additional cyclic products involving the reactive groups during thermal curing could also contribute to the network rigidity by further increasing the number of rigid rings, the bonds between them, and hence the steric crowding effects. Besides, the hindering effect on chromophore relaxation is favored by the optimal position of cross-linking functions, located at both ends of the rod-like molecule. Indeed, the reported procedure was applied to similar trihydroxylated NLO chromophores obtaining analogous results in terms of long-term retention of second-order nonlinearity. To our knowledge, this is one of few examples in the literature where a NLO material with real high performance, in terms of activity and even more of stability, can be obtained with a very simple, quick, and inexpensive process. Due to the matching of these favorable characteristics, we reckon this type of approach to be really competitive for the production of organic-based NLO devices.

4. CONCLUSIONS

A trihydroxylated NLO azochromophore was synthesized, characterized, and functionalized by a reaction with TDI. Treatment of the resulting compound with small amounts of *N*,*N*-dimethylacetamide in THF or dichloromethane and spin coating onto glass or silicon substrates gives amorphous and transparent thin films which cross-link upon thermal curing at 160 °C. The absence of hydroxylated monomers excludes a classical reaction path between isocyanates and hydroxyls to form a polyurethane network, while the formation of cyclic species involving isocyanates and urethanes groups is likely to occur for the effect of DMAC. Samples were successfully and efficiently corona poled during thermal treatment, leading to EO films with good quality and transparency. Measurements of optical nonlinearity by means of SH generation experiments gave values of 33.0 and 10.8 pm/V, respectively, for d_{33} and d_{31} components of second-order nonlinear susceptibility. The main advantage of this cross-linking approach is represented by a very high stability of chromophore orientation and hence of optical nonlinearity. This was demonstrated by aging tests in air on poled samples, which show no appreciable decrease of SHG up to a temperature of 130 °C for a long period and by dynamic thermal stability tests, which evidenced the depoling onset to be shifted 30 °C above. These outstanding properties could be positively exploited for NLO applications, as for example for stable and responsive EO modulators, also considering the scheme for the production of EO films here described, which is actually competitive and viable as well as easy and relatively unexpensive. Furthermore, being the poled film thermally stable and completely insoluble after the cross-link, this route also provides a desirable active medium for subsequent layers deposition/etching treatments usually needed for EO device fabrication.

AUTHOR INFORMATION

Corresponding Author

*Phone: +39 081 674446. Fax: +39 081 674367. E-mail: fabio.borbone@unina.it.

REFERENCES

(1) Burland, D. M.; Miller, R. D.; Walsh, C. A. *Chem. Rev.* **1994**, *94*, 31–75.

(2) Gebremichael, F.; Kuzyk, M. G.; Lackritz, H. S. *Prog. Polym. Sci.* **1997**, *22*, 1147–1201.

(3) Wolff, J. J.; Wortmann, R. *Adv. Phys. Org. Chem.* **1999**, *32*, 121–217.

(4) Prasad, P. N.; Williams, D. J. *Introduction to Nonlinear Optical Effects in Molecules and Polymers*; John Wiley and Sons: New York, 1991.

(5) Raimundo, J. M.; Blanchard, P.; Planas, N. G.; Merrier, N.; Ledoux-Rak, I.; Hierle, R.; Roncali, J. *J. Org. Chem.* **2002**, *67*, 205–218.

(6) Ma, X.; Ma, F.; Zhao, Z.; Song, N.; Zhang, J. *J. Mater. Chem.* **2010**, *20*, 2369–2380.

(7) Li, Q.; Lu, C.; Zhu, J.; Fu, E.; Zhong, C.; Li, S.; Cui, Y.; Qin, J.; Li, Z. *J. Phys. Chem. B* **2008**, *112* (15), 4545–4551.
(8) Borbone, F.; Carella, A.; Ricciotti, L.; Tuzi, A.; Roviello, A.; Barsella, A. *Dyes Pigm.* **2011**, *88*, 290–295.
(9) Rommel, H. L.; Robinson, B. H. *J. Phys. Chem. C* **2007**, *111*, 18765–18777.
(10) Ronchi, M.; Orbelli Biroli, A.; Marinotto, D.; Pizzotti, M.; Ubaldi, M. C.; Pietralunga, S. M. *J. Phys. Chem. C* **2011**, *115*, 4240–4246.
(11) Kim, T.-D.; Luo, J.; Cheng, Y.-J.; Shi, Z.; Hau, S.; Jang, S.-H.; Zhou, X.-H.; Tian, Y.; Polishak, B.; Huang, S.; et al. *J. Phys. Chem. C* **2008**, *112*, 8091–8098.
(12) Li, Z.; Wu, W.; Ye, C.; Qin, J.; Li, Z. *J. Phys. Chem. B* **2009**, *113*, 14943–14949.
(13) Kang, J.-W.; Kim, T.-D.; Luo, J.; Haller, M. *Appl. Phys. Lett.* **2005**, *87*, 071109/1–071109/3.
(14) Kim, T.-D.; Kang, J.-W.; Luo, J.; Jang, S.-H.; Ka, J.-W.; Tucker, N.; Benedict, J. B.; Dalton, L. R.; Gray, T.; Overney, R. M.; et al. *J. Am. Chem. Soc.* **2007**, *129*, 488–489.
(15) Enami, Y.; Mathine, D.; Derose, C. T.; Norwood, R. A.; Luo, J.; Jen, A. K.-Y.; Peyghambarian, N. *Appl. Phys. Lett.* **2007**, *91*, 093505/1–093505/3.
(16) Cui, Y.; Qian, G.; Chen, L.; Wang, Z.; Gao, J.; Wang, M. *J. Phys. Chem. B* **2006**, *110*, 4105–4110.
(17) Yu, J.; Cui, Y.; Gao, J.; Wang, Z.; Qian, G. *J. Phys. Chem. B* **2009**, *113*, 14877–14883.
(18) Verbiest, T.; Burland, D. M.; Jurich, M. C.; Lee, V. Y.; Miller, R. D.; Volksen, W. *Science* **1995**, *268*, 1604–1606.
(19) Saadeh, H.; Yu, D.; Wang, L. M.; Yu, L. P. *J. Mater. Chem.* **1999**, *9*, 1865–1873.
(20) Chen, T. A.; Jen, A. K.-Y.; Cai, Y. M. *J. Am. Chem. Soc.* **1995**, *117*, 7295–7296.
(21) Davey, M. H.; Lee, V. Y.; Wu, L.-M.; Moylan, C. R.; Volksen, W.; Knoesen, A.; Miller, R. D.; Marks, T. J. *Chem. Mater.* **2000**, *12*, 1679–1693.
(22) Borbone, F.; Caruso, U.; De Maria, A.; Fusco, M.; Panunzi, B.; Roviello, A. *Macromol. Symp.* **2004**, *218*, 313–321.
(23) Haller, M.; Luo, J.; Li, H.; Kim, T.-D.; Robinson, B. H.; Jen, A. K.-Y. *Macromolecules* **2004**, *37*, 688–690.
(24) Kim, T. D.; Luo, J.; Ka, J.-W.; Hau, S.; Tian, Y.; Shi, Z.; Tucker, N. M.; Jang, S.-H.; Kang, J.-W.; Jen, A. K.-Y. *Adv. Mater.* **2006**, *18*, 3038–3042.
(25) Shi, Z.; Luo, J.; Huang, S.; Cheng, Y.-J.; Kim, T.-D.; Polishak, B. M.; Zhou, X.-H.; Tian, Y.; Jang, S. H.; Knorr, D. B., Jr.; et al. *Macromolecules* **2009**, *42*, 2438–2445.
(26) Borbone, F.; Caruso, U.; Diana, R.; Panunzi, B.; Roviello, A.; Tingoli, M.; Tuzi, A. *Org. Electron.* **2009**, *10*, 53–60.
(27) Boogers, J. A. F.; Klaase, P. T. A.; De Vlieger, J. J.; Alkema, D. P. W.; Tinnemans, A. H. A. *Macromolecules* **1994**, *27*, 197–204.
(28) Boogers, J. A. F.; Klaase, P. T. A.; De Vlieger, J. J.; Tinnemans, A. H. A. *Macromolecules* **1994**, *27*, 205–209.
(29) Carella, A.; Centore, R.; Mager, L.; Barsella, A.; Fort, A. *Org. Electron.* **2007**, *8*, 57–62.
(30) Zhang, C.; Wang, C.; Dalton, L. R.; Zhang, H.; Steier, W. H. *Macromolecules* **2001**, *34*, 253–261.
(31) Lapprand, A.; Boisson, F.; Delolme, F.; Méchin, F.; Pascault J.-P. *Polym. Degrad. Stab.* **2005**, *90*, 363–373.
(32) Dyer, E.; Majewski, T. E.; Nycz, T. J.; Travis, J. D. *J. Heterocycl. Chem.* **1972**, *9*, 955–958.
(33) Matsui, T.; Kamatani, H.; Arimatsu, Y.; Kaji, A.; Hattori, K.; Suzuki, H. *J. Appl. Polym. Sci.* **1991**, *42* (9), 2443–2452.
(34) Zyss, J.; Chemla, D. S. *Nonlinear Optical Properties of Organic Molecules and Crystals*, Vol. 1; Academic Press: New York, 1987.
(35) Caruso, U.; Casalboni, M.; Fort, A.; Fusco, M.; Panunzi, B.; Quatela, A.; Roviello, A.; Sarcinelli, F. *Opt. Mater.* **2005**, *27*, 1800–1810.
(36) Maker, P. D.; Terhune, R. W.; Nisenoff, M.; Savage, C. M. *Phys. Rev. Lett.* **1962**, *8*, 21–22.
(37) El Ouazzani, H.; Iliopoulos, K.; Pranaitis, M.; Krupka, O.; Smokal, V.; Kolendo, A.; Sahraoui, B. *J. Phys. Chem. B* **2011**, *115*, 1944–1949.
(38) Herman, W. N.; Hayden, L. M. *J. Opt. Soc. Am. B* **1995**, *12* (3), 416–427.
(39) Shoji, I.; Kondo, T.; Ito, R. *Opt. Quant. Electron.* **2002**, *34*, 797–833.
(40) Xie, H.; Wei, J.; Zhang, X. *J. Phys.: Conf. Ser.* **2006**, *28*, 95–99.
(41) Jellison, G. E., Jr.; Modine, F. A. *Appl. Phys. Lett.* **1996**, *69*, 371–373.
(42) Kleinman, D. A. *Phys. Rev.* **1962**, *126*, 1977–1979.
(43) Williams, D. J. Nonlinear optical properties of guest-host polymer structures. In *Nonlinear Optical Properties of Organic Molecules and Crystals*; Chemla, D. S., Zyss, J., Eds.; Academic Press: Orlando, FL, 1987; pp 405−435.